available at www.sciencedirect.com

www.elsevier.com/locate/fuproc

Devolatilization of coals of North-Eastern India under fluidized bed conditions in oxygen-enriched air

R.C. Borah[a,b,*], P. Ghosh[b], P.G. Rao[a]

[a]Chemical Engineering Division, North East Institute of Science and Technology, Jorhat -785006, India
[b]Department of Chemical Engineering, Indian Institute of Technology Guwahati, Guwahati-781039, India

ARTICLE DATA

Article history:
Received 4 January 2008
Received in revised form 4 June 2008
Accepted 15 July 2008

Keywords:
Cost analysis
Devolatilization
Fluidized bed
Oxygen-enriched air
Shrinking-core model

ABSTRACT

Oxygen-enriched air can increase the combustion efficiency, boiler efficiency, and sulfur absorption efficiency of atmospheric fluidized bed combustion (AFBC) boilers which use high-sulfur coal, and other combustion systems that use coal. Devolatilization is the first step in the gasification or combustion of coal. In this work, devolatilization characteristics of five run-of-mine (ROM) coals of North-Eastern India having particle-size between 4 mm and 9 mm are reported. The experiments were performed under fluidized bed conditions at 1123 K in enriched air containing 30% oxygen. The devolatilization time was correlated with the particle diameter by a power law correlation. The variation of mass with time was correlated by an exponential correlation. It was observed that the average ratio of yield of volatile matter to the proximate volatile matter decreased with the increase in volatile-content of the coals. A shrinking-core model was used to determine the role of film-diffusion, ash-diffusion and chemical reaction. The experimental results indicate the likelihood of film-diffusion to be the rate-controlling mechanism in presence of oxygen-enriched air. A cost-analysis was carried out to study the economy of the process.

1. Introduction

Fluidized bed combustion and gasification are two recognized technologies for the utilization of coals containing high amounts of sulfur and ash. Amongst the fluidized bed technologies, atmospheric fluidized bed combustion (AFBC) is simple and economical because it can use particles of large size, offers flexibility in the type of the fuel used, and reduces erosion and corrosion. Though the other types of fluidized bed, i.e., pressurized and circulating fluidized beds are more efficient in combustion as well as sulfur-capture because of lower particle size, higher recirculation rate, and presence of higher amount of air, yet the costs of production are comparatively higher than AFBC. By the application of oxygen-enriched air in AFBC, the deficiency in combustion and thermal efficiency can be removed, and can be made at par with the pressurized and circulating fluidized bed combustors. In oxygen-enriched environment, devolatilization and combustion of coal particles are likely to occur faster than that with air. Also, there occurs increase in combustion of coal char and volatiles because of the presence of extra oxygen in the combustion system, which increases the combustion efficiency [1,2]. Thermal efficiency of the system also increases due to the reduction of the total volume of the flue gas leaving the combustion chamber [3]. Oxygen-enriched combustion method is an effective method to produce a flue gas rich in carbon dioxide which can be separated easily [4,5] and sequestered [6]. It is also known that the use of oxygen-enriched air and recycle of char help a gasifier to increase the heating value of the

* *Corresponding author*. Chemical Engineering Division, North East Institute of Science and Technology, Jorhat-785006, India. Tel.: +91 376 2370117x2383; fax: +91 376 2370011.
E-mail address: borahrc@rrljorhat.res.in (R.C. Borah).

0378-3820/$ – see front matter
doi:10.1016/j.fuproc.2008.07.011

product gas and cold gas efficiency. The ratio of conversion of carbon to CO_2 and CO increases with the increase of oxygen concentration in the combustion chamber [7]. Air enriched with oxygen can reduce the emission of carbon monoxide in the flue gas of a fluidized bed combustor. In some works, secondary air was injected for combustion of volatiles in the free-board to bring the emission of carbon monoxide below the pollution limit [8]. The amount of unburned carbon in the flue gas reduces considerably in presence of extra oxygen. However, the cost for oxygen-enrichment is higher, owing to the cost involved in the liquefaction of air [9].

Combustion studies related to pulverized coal with enriched air have revealed that there is an increase in the flux of oxygen molecules from the bulk towards the particles. As a result, the temperature of the surface of the particles becomes higher. This increases the pyrolysis rate, Stefan flow and oxidation in the boundary layer [10]. But there is a difference between higher oxygen concentration and higher excess-air condition; the latter leads to a higher fluidization velocity. At higher fluidization velocities the rate of release of volatile matter is slightly higher because of the better convective heat transfer to the particle [11]. As nitrogen does not participate in combustion, at higher fluidization velocities, the volume of nitrogen is quite high and the sensible heat is lost, which is carried away by the excess nitrogen.

During the heating process of the coal particles in fluidized bed, the average heating rate of the individual coal particles depends on their size. From the data reported in literature [12] it is observed that the average heating rate of large particles is lower than the average heating rate of small particles. It is also reported that the differences in temperature history of the center of the coal particles are mostly influenced by the type of coal and the particle size [13].

Heat transferred from the fluidized bed media to the coal particle is utilized in the drying of the coal particle and the endothermic reactions leading to the formation of the volatiles. Exothermic reactions in the combustion of char cause increase in the temperature of the particle and thereby increase heat transfer from the particle to the surrounding medium. Increase in particle temperature increases the rate of drying and devolatilization of coal. In presence of excess oxygen, exothermic reactions release sensible heat from the combustion of volatiles and char. This can accelerate drying and formation of volatiles. Hence it is important to study devolatilization of coal of different particle size relevant to fluidized bed under enriched-oxygen conditions.

Devolatilization is a general term signifying the removal of volatile matters from the coal matrix. It is stated that pyrolysis-like conditions are encountered by the coal particles prior to ignition even under oxidizing conditions [14]. From the foregoing discussions it is evident that the increase in oxygen concentration in the fluidizing gas increases the exothermic reactions as well as the devolatilization rate. Hence the characteristics of devolatilization are not similar in inert atmosphere, air, and air enriched with oxygen. In the present work, we have studied coals of five collieries located in the North-Eastern part of India. Particles having diameter between 4 mm and 9 mm were studied. The continuous loss of mass was measured in oxygen-enriched (30% oxygen in the air) environment under fluidized bed conditions. From these data, the characteristics of devolatilization of large coal particles in oxygen-enriched environment were determined quantitatively.

2. Experimental

2.1. *Devolatilization time*

In this work, *devolatilization time* is defined as the point of intersection of the two linear portions of the mass versus time curve [15]. It is known that the methods by which the end of devolatilization in fluidized bed combustor is determined can influence the results [16]. Some of these are explained as follows. Visual detection of the disappearance of a visible flame around the coal particles at the bed surface may be erroneous due to the varying residence times of different particles in the bed. The measurement of mass of the particle by interrupting the process can also lead to erroneous results because the devolatilization process continues up to the moment of the actual measurement. When the temperature of the combustion products is measured, estimates of the end of the combustion of the volatiles can be seriously in error.

2.2. *Analysis of the coal samples*

The proximate and ultimate analyses of the coal samples were carried out by the methods outlined in IS: 1350 and IS: 1351, respectively. The calorific values were determined using the methods prescribed in IS: 1350. The results of these analyses are presented in Table 1.

2.3. *Determination of particle diameter*

A range of particle mass (e.g., 0.145 g–0.155 g) was chosen for each of the coal samples to obtain the mass-equivalent-volumetric diameter. In each range, about 20 coal particles were present. The diameters of the particles studied in this work were between 4 and 9 mm, as mentioned in Section 1. The density was determined by estimating the volume of water displaced, as per the procedure described in ASTM D854-06. While calculating the volume of water, the density corrections corresponding to the room temperature were taken into account. About fifty coal particles for each size range were collected and dried in an electric oven in nitrogen atmosphere for 1 h at 378 K. They were preserved in sealed bottles for future analysis so that they were not oxidized by air.

2.4. *Experiments on devolatilization*

The devolatilization apparatus used to carry out the experiments was similar to the apparatus used in literature [17]. It is shown in Fig. 1. Instead of a gas pre-heater, the fluidized bed was used to raise the temperature of the fluidizing media to the desired temperature as described by Zabrodsky [18]. The fluidized bed consisted of a cylindrical tube made of sillimanite having 25 mm internal diameter and 600 mm length. It was housed inside a mild steel casing, which was packed with

Table 1 – Proximate and ultimate analyses of the coal samples

Analysis	Parameter (%)	Colliery				
		Baragolai	Ledo	Tikak	Baragolai A	Tirap
Proximate analysis (air-dried)	Volatile matter	31.2	40.8	37.8	35.4	38.1
	Fixed carbon	36.5	46.9	43.8	43.0	45.6
	Ash	28.8	10.1	16.7	19.3	14.4
	Moisture	3.5	2.2	1.7	2.3	1.9
	Gross specific energy (MJ/kg)	21.39	28.97	27.3	25.6	28.07
Ultimate analysis (daf)	Carbon	81.0	79.9	81.0	80.4	81.6
	Hydrogen	5.7	5.7	5.8	6.0	5.3
	Nitrogen	1.5	1.4	1.1	1.3	1.3
	Sulfur	4.0	4.6	3.5	5.4	4.9
	Oxygen (by difference)	7.8	8.4	8.6	6.9	6.9

insulating brick. The casing had 20 cm diameter and was 60 cm long. The total resistance of the heating element [make: Kanthal (UK)] was 55 Ω, which delivered a maximum of 1 kW power. The furnace had provisions for heating up to 1273 K. Digital temperature controllers [make: Max-Thermo (Taiwan)] were used for recording and controlling the temperature of the furnace. A steel tube of 19 mm diameter and 101.6 mm height having perforations of 2 mm diameter at its periphery (~3% open area) was used as the gas distributor at the bottom of the cylindrical sillimanite tube. Calcined lime particles of approximately 0.72 mm diameter were used as the bed material for fluidization. The minimum fluidization velocity of the bed material was 0.53 m/s. High purity moisture-free air and oxygen were mixed such that oxygen concentration in the mixed air was 30%. The air and oxygen were supplied to the system directly from two gas cylinders. The flow rates of the gases were measured by rotameters. An online Zirconia oxygen gas analyzer [make: Fuji Electric Co. (Japan)] having response time of 10 s was used to monitor the oxygen concentration of air. A water manometer was connected to the gas line to measure the pressure drop across the rotameter.

The coal particle under investigation was held in a basket of 12 mm diameter and 20 mm height. It was made of a platinum–rhodium net, and was suspended with the help of a platinum wire from the hook of a microbalance [make: AND (Japan)]. The response time of the microbalance was 0.3 s. The microbalance was connected to a personnel computer via the RS-232 data interface. The data-capturing software enabled us to record the weight measured by the balance in a continuous manner. The position of the suspended basket was such that when the vertical furnace was lifted with the help of the lifting device, the coal particle in the basket was placed just above the fluidized bed and experienced the conditions of the hot furnace instantly, as a particle would experience in a typical fluidized bed. A chromel–alumel thermocouple was inserted into the freeboard section of the bed to measure the temperature as well as to control the furnace temperature. It was inserted to such a depth that it was positioned just above the expanded bed.

Initially, the power input to the electric coil was adjusted to give a uniform temperature (1123 K) inside the furnace. After this, purging of the enriched air was commenced. It was

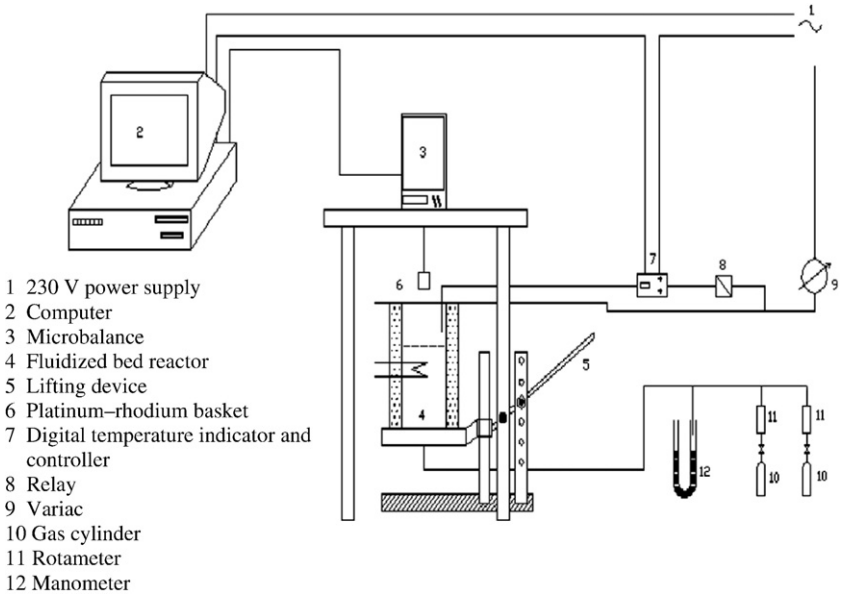

Fig. 1 – Experimental setup used for the devolatilization studies.

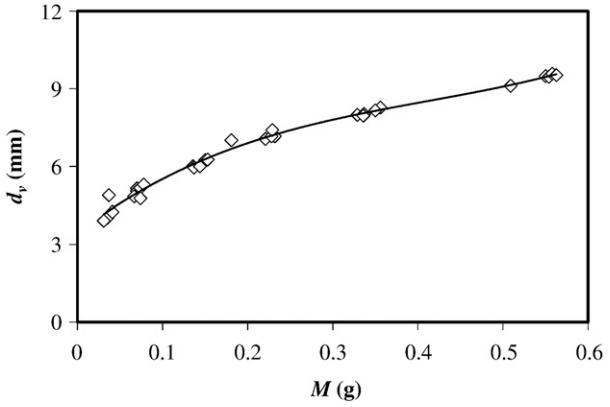

Fig. 2 – Dependence of mass-equivalent-volumetric diameter (d_v) on the mass of the particle (M) for the five coals.

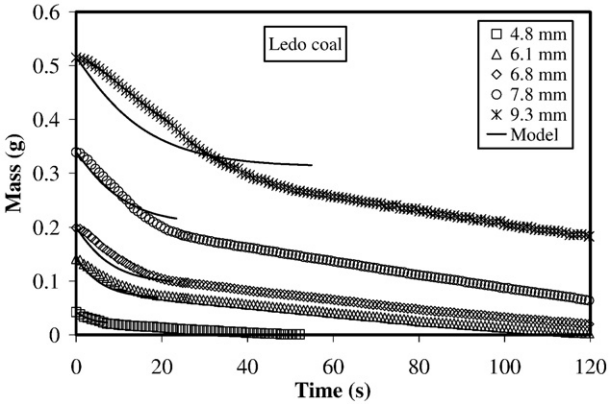

Fig. 4 – Mass vs. time profiles of Ledo coal for different particle size.

adjusted such that the velocity of the fluidizing gas was 1 m/s. Once the velocity of the gas and the temperature were stabilized, the empty basket with the platinum wire was suspended from the balance hook and the furnace assembly was lifted with the help of the lifting device as described before. The empty run was recorded and the furnace was lowered. As soon as the empty basket and the platinum wire assembly cooled down to room temperature, the pre-weighed coal sample was put into the basket. The furnace assembly was lifted with the help of the lever and the system was locked at that position. The weight was recorded continuously. The time versus weight data were analyzed.

3. Results and discussion

3.1. *Determination of the mass-equivalent-volumetric diameter (d_v)*

The mass–equivalent–volumetric diameter (assuming the coal particles to be spherical) was calculated following the procedure given in the literature [19], and described in Section 2.3. The average diameter was plotted against the average mass of the particles for all five coal samples, as shown in Fig. 2. The data were fitted by the following polynomial equation.

$$d_v = 37.51M^3 - 46.35M^2 + 25.10M + 3.43 \quad (1)$$

where M is the mass of the coal particle. Eq. (1) fitted the data well (coefficient of determination, $R^2 = 0.99$).

3.2. *Analysis of the data on devolatilization time*

The mass of the particles of five coals of different size during devolatilization in enriched air with respect to time are given in Figs. 3–7. It can be observed from these figures that the curves consist of two distinct linear segments. The first segment is due to devolatilization and the second segment is due to char combustion. In this paper, only the devolatilization segments were analyzed. Fragmentation of particles was not observed in any of the experiments. Devolatilization time (as defined in Section 2.1) t_v was correlated with the particle diameter d_v as $t_v = Ad_v^n$, where A and n are constants.

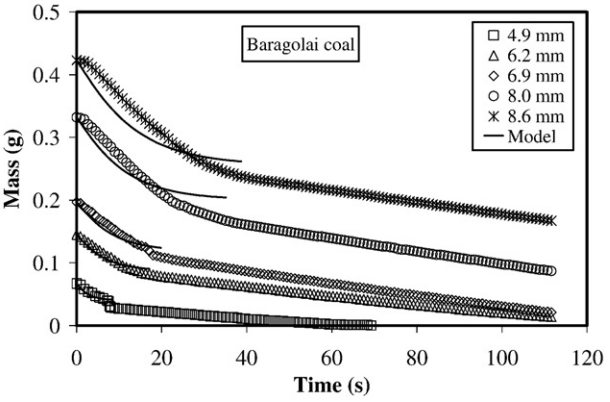

Fig. 3 – Mass vs. time profiles of Baragolai coal for different particle size.

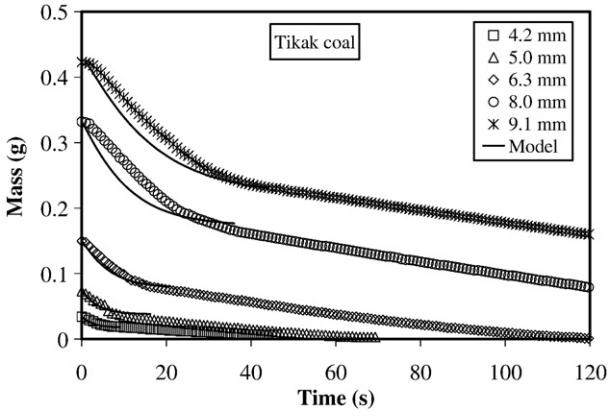

Fig. 5 – Mass vs. time profiles of Tikak coal for different particle size.

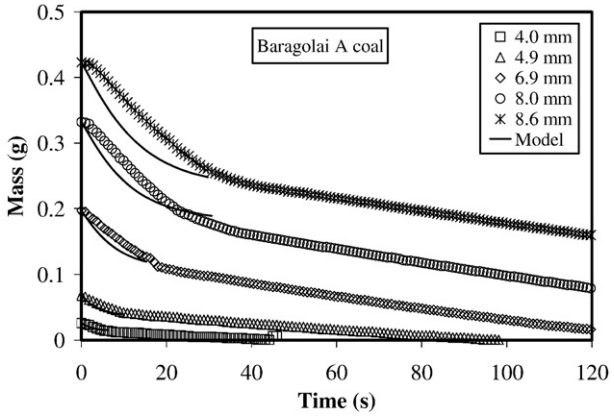

Fig. 6 – Mass vs. time profiles of Baragolai A coal for different particle size.

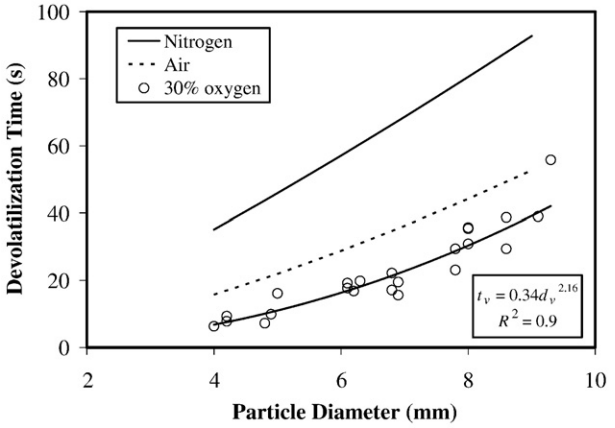

Fig. 8 – Comparison of devolatilization time in fluidized bed at 1123 K in different atmospheres.

Regressing the data from all coal samples (Fig. 8), it was found that $A=0.34$ and $n=2.16$. There is no work reported in the literature on devolatilization of coal under fluidized bed conditions in presence of oxygen-enriched air. However, there are reports on devolatilization in presence of inert gas [12,20] and air [12,19,21–23]. The present data appear to be reasonable in comparison with these results. In oxidizing atmosphere, there is reduction in the devolatilization time because of the increase of surface temperature by the combustion of volatiles at the surface. The correlations reported in the literature for inert gas as well as air differ from one another considerably. The probable reason for this difference lies in the type of coal used, and the experimental methods attempting to simulate the fluidized bed conditions. Best-fit correlations were derived using these correlations. For inert atmosphere, we found $A=6.684$ and $n=1.197$, and for air we found $A=2.08$ and $n=1.47$. From Fig. 8 it can be observed that the devolatilization time decreased with increase in concentration of oxygen. It was found that A decreased linearly with the concentration of oxygen (C_{O_2}) as given by the correlation:

$$A = -0.2195 C_{O_2} + 6.9155, \quad R^2 = 0.99 \tag{2}$$

and n increased with increase in oxygen concentration following the correlation:

$$n = 9 \times 10^{-5} C_{O_2}^3 - 2.7 \times 10^{-3} C_{O_2}^2 + 0.0276 C_{O_2} + 1.197, \quad R^2 = 1 \tag{3}$$

The correlations given by Eqs. (2) and (3) are shown in Fig. 9. Most of the values of A and n reported in the literature vary between 4 and 10, and 1 and 1.5, respectively, for devolatilization in inert atmosphere. Similarly, most of the values of A and n vary between 1.5 and 4.5, and 1.1 and 1.8, respectively, for devolatilization in air. The values of A and n reported by Salam et al. [23] for a fluidizing gas containing 3% oxygen differ widely from the values reported in the other works. These values were not considered in developing the correlations given by Eqs. (2) and (3). It is evident from Figs. 8 and 9 that the oxygen-content in the fluidizing gas has considerable effect on the devolatilization time. With increase in concentration of

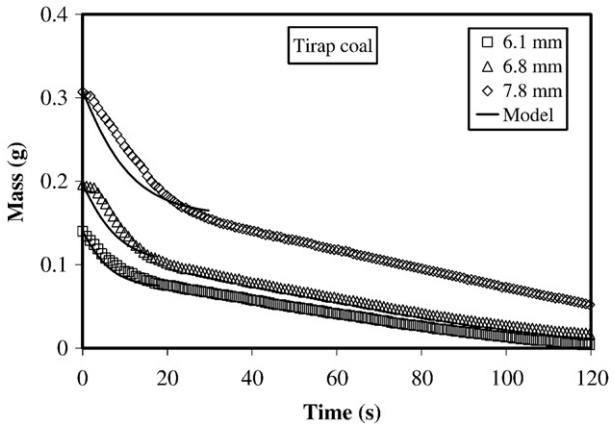

Fig. 7 – Mass vs. time profiles of Tirap coal for different particle size.

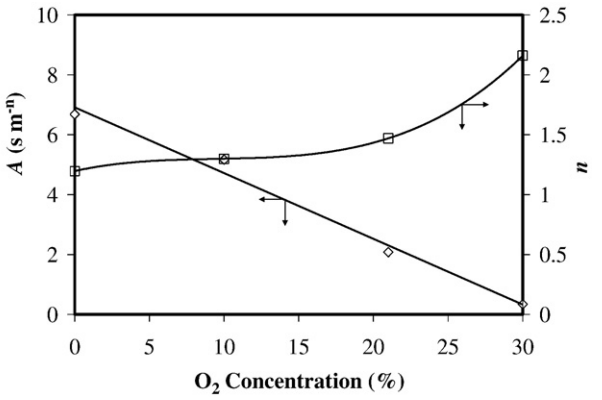

Fig. 9 – Variation of the parameters A and n with oxygen concentration in the fluidizing gas.

oxygen in the gas, the concentration gradient of oxygen increased. This resulted in more diffusion of oxygen through the gas film surrounding the particle. With the increase in diffusion of oxygen, reaction was enhanced and the release of sensible heat increased. Thus, the loss of volatiles was faster.

The fractional loss of mass [i.e., the fractional release of volatile matter at time t, $v(t)$] with fractional time (ζ) was fitted by a simple profile,

$$v(t) = 1 - exp(-b\zeta^m) \quad (4)$$

where, b and m are constants. These constants were obtained by fitting the experimental data involving coals from five collieries having a wide range of size. $v(t)$ is defined as,

$$v(t) = \frac{V - V_0}{V_\infty - V_0} \quad (5)$$

where, V is the mass at any time, and V_0 and V_∞ represent the total mass before and after devolatilization, respectively. The fractional time ζ is defined as,

$$\zeta = \frac{t}{t_v} \quad (6)$$

The values of b and m were determined by minimizing the mean square average deviation (Δ), defined as,

$$\Delta = \frac{\sum \left[v(t)_{Expt} - v(t)_{Model}\right]^2}{N} \quad (7)$$

where, $v(t)_{Expt}$ is the experimental value of the fraction devolatilized, $v(t)$ model is the value of the fraction devolatilized predicted by the Eq. (4) and N is the number of data points. The values of b and m were found to be 3.15 and 1.1, respectively, for the coals used in this study. Eq. (4) can be converted to a generalized correlation between the fractional release of volatile matter $v(t)$ and the elapsed time (t) as,

$$v(t) = 1 - exp(-ct^m), \quad 0 \le t \le t_v \quad (8)$$

where, c is related to t_v by the following equation.

$$c = \frac{b}{(t_v)^m}, \quad b = 3.15, m = 1.1 \quad (9)$$

The ratio of the yield of volatile matter to the proximate volatile matter has been found to vary between 0.83 and 1.86

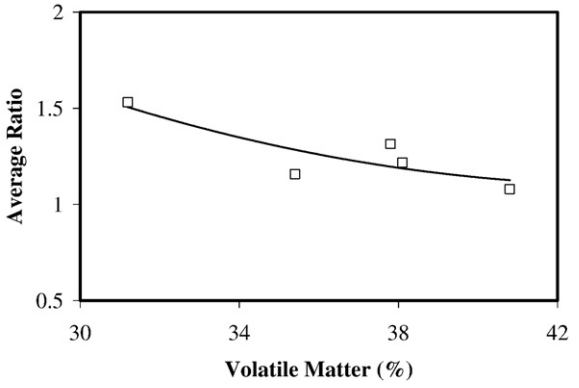

Fig. 10 – Variation of the ratio of yield of devolatilization to proximate volatile matter with the volatile matter of the coals.

Table 2 – Experimental results

Colliery	Size (mm)	Total devolatilization time (s)	Yield of devolatilization (%)	Proximate volatile matter (%)	Ratio of yield of volatile matter to proximate volatile matter	c(s^{-m})	$\Delta \times 10^2$
Baragolai	4.2	9.3	58.2	31.2	1.86	0.341	0.72
	6.2	16.8	43.5		1.39	0.135	0.60
	6.9	19.5	44.2		1.42	0.105	0.89
	8.0	35.4	49.7		1.59	0.074	2.03
	8.6	38.7	43.7		1.40	0.062	2.45
Ledo	4.8	7.2	50.0	40.8	1.23	0.248	0.12
	6.1	19.2	34.0		0.83	0.140	1.13
	6.8	22.2	49.8		1.22	0.108	1.40
	7.8	23.1	37.2		0.91	0.078	1.44
	9.3	55.8	49.3		1.21	0.052	3.56
Tikak	4.2	7.8	44.1	37.8	1.19	0.341	0.18
	5.0	16.1	60.3		1.59	0.225	0.56
	6.3	19.8	49.3		1.31	0.130	0.64
	8.0	35.7	50.0		1.32	0.074	2.13
	9.1	39.0	44.0		1.16	0.054	3.15
Baragolai A	4.0	6.3	46.2	35.4	1.30	0.382	0.15
	4.9	9.9	38.2		1.08	0.236	0.61
	6.9	15.6	35.5		1.00	0.105	1.31
	8.0	30.9	47.0		1.33	0.074	1.86
	8.6	29.4	38.3		1.08	0.062	3.57
Tirap	6.1	17.7	45.0	38.1	1.18	0.140	0.68
	6.8	17.1	44.9		1.18	0.108	1.45
	7.8	29.4	49.2		1.29	0.078	1.73

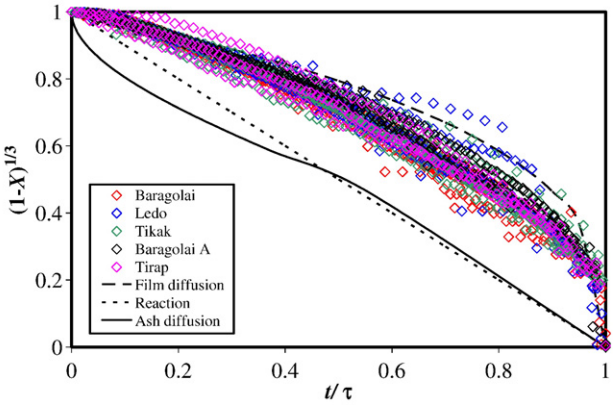

Fig. 11 – Variation of $(1-X)^{1/3}$ with t/τ for the experimental data, and the different controlling mechanisms according to the shrinking-core model.

(Table 2). The average ratio for 23 coal samples was found to be 1.264.

Eqs. (5) and (8) can be used to determine the mass of a single coal particle at any instant until the completion of devolatilization, as shown below.

$$V = V_0 + (V_\infty - V_0)[1 - exp(-ct^m)], \quad 0 \le t \le t_v \tag{10}$$

The total yield of volatile matter, $(V_0–V_\infty)$, can be taken as 1.264 times the proximate volatile-content of the coal. The mass of coal samples as calculated by Eq. (10) is shown by the lines in Figs. 3–7. The mean square average deviations for each particle size are given in Table 2.

The ratio of the yield of volatile matter to proximate volatile matter (Table 2, column 6) decreased with the increase in volatile-content of the coals. The average values of the ratio (for the coal samples of one colliery) have been plotted against the volatile-content of the coals, as shown in Fig. 10. It can be observed from this figure that the ratio showed a decreasing trend with the increase in volatile-content. Similar observations can be made from the results reported in literature [17,24,25]. This is probably because of the difference in specific heat of the coals with different volatile-content. The specific heat of the low-volatile coals is lower than the specific heat of the high-volatile coals [26]. The rate of increase of temperature of the low-volatile coals is higher than the high-volatile coals. In our experiments, the effective rate of heating was quite high due to the presence of oxygen. It has been reported in the literature [27] that the rapid increase of temperature during high heating-rate decreases the residence time of volatile matter, diminishes the influence of cracking, and more tarry liquid is produced. The yield of light hydrocarbon gases, however, remains nearly constant. It has also been reported in literature [27] that the increase in the yield of tar with increase in heating rate is higher for the low-volatile coals than that for the high-volatile coals, which also supports the fact that low-volatile coals are heated more rapidly than the high-volatile coals. Therefore, the residence time of volatile matter of the low-volatile coals is lower than that of the high-volatile coals, which is reflected in the higher yield of volatile matter for the low-volatile coals. Therefore, the ratio decreased with the increase in volatile-content of the coals.

It has been shown in the literature that devolatilization of coal can be modeled by the shrinking-core model with no change in the size of the particle [28]. The value of the exponent n (≅2.16) suggests that coal devolatilization in enriched air is either ash-diffusion or film-diffusion controlled [29]. To find out the rate-controlling step of devolatilization (i.e., whether film-diffusion, chemical reaction, or ash-diffusion is the controlling mechanism) we have calculated the

Table 3 – Comparison of cost involved in various combustion technologies

Sl. No.	Technology	Cost	Plant efficiency	CO_2 emission	SO_2 emission	NO_x emission	Particulate emission
		(Canadian $/MWh)	(%)	(kg/MWh)	(kg/MWh)	(kg/MWh)	(kg/MWh)
01	Subcritical pulverized coal combustion	43.30	33	1000	1.6	2.1	0.5
02	Supercritical pulverized coal combustion	42.94	38–43	870–770	1.4	1.8	0.4
03	Atmosphere fluidized bed combustion	42.45	36	920	0.3	0.5	~0.4
04	Atmospheric fluidized bed combustion with 30% oxygen-containing air	44.91	n/a	n/a	n/a	n/a	n/a
05	Pressurized fluidized bed combustion	45.58	42	790	0.1	<0.7	0.1–0.5
06	Integrated gasification combined cycle	46.04	45	735	~0.0	0.3–0.5	~0.0

fractional conversion at any point of time using the following equations [29]:

$$\frac{t_{\text{film alone}}}{\tau_{\text{film alone}}} = X \tag{11}$$

$$\frac{t_{\text{reaction alone}}}{\tau_{\text{reaction alone}}} = \left[1-(1-X)^{1/3}\right] \tag{12}$$

$$\frac{t_{\text{ash diffusion alone}}}{\tau_{\text{ash diffusion alone}}} = \left[1-3(1-X)^{2/3}+2(1-X)\right] \tag{13}$$

where, $t_{\text{ash diffusion alone}}$ is the time of devolatilization for any conversion considering ash-diffusion controlling alone, $t_{\text{film alone}}$ is the time of devolatilization for any conversion considering film-diffusion controlling alone, and $t_{\text{reaction alone}}$ is the time of devolatilization for any conversion considering reaction controlling alone. The τ -terms ($\equiv t_v$) represent the times of devolatilization for complete conversion. X is the fraction converted in time t. The fractional conversion, X, is defined as,

$$X = \frac{V_0 - V}{V_0 - V_\infty} \tag{14}$$

For the spherical particles of constant size,

$$X = 1-(d_c/d_v)^3 \tag{15}$$

where, d_c is the diameter of the unreacted core. The predictions from the shrinking-core model by Eqs. (11)–(13) have been compared with the experimental data in Fig. 11. It can be observed from this figure that the experimental data lie close to the film-diffusion model (Eq. (11)). Therefore, it is likely that film-diffusion is the controlling mechanism.

4. Cost analysis

Approximate capital cost of our system was calculated using the data presented by M/S Alstom Power Inc. [9]. The unit costs were compared with the data given by Wong and Whittingham [30], as shown in Table 3. From this table it can be observed that the unit cost of the AFBC system is lowest. When an AFBC is upgraded with additional requirement of oxygen (as in our system) the unit cost becomes higher than the subcritical and supercritical pulverized coal combustion systems, and the atmospheric fluidized bed combustion system. However, the cost is lower than the pressurized fluidized bed combustion system and integrated gasification combined cycle. Since the devolatilization time in oxygen-enriched air is shorter in comparison with air (as shown in our study) the combustion efficiency and boiler efficiency are likely to be higher than that in AFBC. The plant-efficiency of our system is anticipated to be marginally lower than AFBC because of the consumption of power for air-separation. A comparative study of CO_2, SO_2, NO_x and particulate emission has also been presented in Table 3.

5. Conclusion

This work has presented new results on devolatilization of coals from five collieries of North-Eastern India in presence of oxygen-enriched air under fluidized bed conditions. It can be concluded from the present study that devolatilization is considerably faster in presence of enriched air having 30% oxygen than inert gas or air. This can increase the combustion efficiency and heat transfer from the bed. Further work is necessary for optimizing the oxygen concentration in the fluidizing gas for optimum devolatilization time.

Devolatilization time (t_v) was correlated with the particle diameter (d_v) by a power law correlation: $t_v = A d_v^n$. The experimental data were fitted well with $A=0.34$ and $n=2.16$. A comparison with other power law correlations reported in the literature in inert gas and air indicated that A decreased and n increased with increase in oxygen-content of the fluidizing gas.

The mass-loss characteristics were studied in enriched air for the five coals having different particle size. An average value of the yield of volatile matter was determined, which was used to calculate the release of volatiles with time theoretically. From the mass- loss characteristics and devolatilization time (determined from its correlation with d_v), it will be convenient to optimize the size range of the feed particles, and the static bed height of a fluidized bed combustor.

The ratio of yield of devolatilization to the proximate volatile matter was found to decrease with the increase in the volatile-content of the coals. It is due to the higher yield of volatile matter for the low-volatile coals than the high-volatile coals. The shrinking-core model was used to study the mechanism of devolatilization. It was found that the experimental data matched closely with the film-diffusion mechanism.

The cost of fluidized bed combustion with 30% oxygen-enriched air was compared with other combustion technologies. It was found that the cost is higher than atmospheric fluidized bed combustion, and subcritical and supercritical pulverized coal combustion technologies. However, the cost is lower than pressurized fluidized bed combustion, and integrated gasification combined cycle technologies.

REFERENCES

[1] Y.Q. Hu, H. Nikzat, M. Nawata, N. Kobayashi, M. Hasatani, The characteristics of coal-char oxidation under high partial pressure of oxygen, Fuel 80 (2001) 2111–2116.
[2] N. Kimura, K. Omata, T. Kiga, S. Takano, S. Shikisima, The characteristics of pulverized coal combustion in O_2/CO_2 mixtures for CO_2 recovery, Energy Conversion and Management 36 (1995) 805–808.
[3] Y. Tan, M.A. Douglas, K.V. Thambimuthu, CO_2 capture using oxygen enhanced combustion strategies for natural gas power plants, Fuel 81 (2002) 1007–1016.
[4] Y.Q. Hu, N. Kobayashi, M. Hasatani, The reduction of recycled-NOx in coal combustion with O_2/recycled flue gas under low recycling ratio, Fuel 80 (2001) 1851–1855.
[5] Y. Hu, S. Naito, N. Kobayashi, M. Hasatani, CO_2, NO_x and SO_2 emissions from the combustion of coal with high oxygen concentration gases, Fuel 79 (2000) 1925–1932.
[6] Y. Tan, E. Croiset, M.A. Douglas, K.V. Thambimuthu, Combustion characteristics of coal in a mixture of oxygen and recycled flue gas, Fuel 85 (2006) 507–512.
[7] T. Czakiert, Z. Bis, W. Muskala, W. Nowak, Fuel conversion from oxy-fuel combustion in a circulating fluidized bed, Fuel Processing Technology 87 (2006) 531–538.

[8] R.C. Borah, B. Mazumder, M.M. Bora, Atmospheric fluidized bed combustion of high sulphur high volatile N. E. region coals of India, Research and Industry 40 (1995) 315–321.
[9] Alstom Power Inc., Greenhouse Gas Emissions Control by Oxygen Firing in Circulating Fluidized Bed Boilers (PPL Report No. PPL-03-CT-09), US Department of Energy, Pennsylvania, 2003, p. 340.
[10] C.A. Gurgel Veras, J. Saastamoinen, J.A. Carvalho Jr., M. Aho, Overlapping of the devolatilization and char combustion stages in the burning of coal particles, Combustion and Flame 116 (1999) 567–579.
[11] F. Winter, M.E. Prah, H. Hofbauer, Temperature in a fuel particle burning in a fluidized bed: the effect of drying, devolatilization, and char combustion, Combustion and Flame 108 (1997) 302–314.
[12] D.P. Ross, C.A. Heidenreich, D.K. Zhang, Devolatilization times of coal particles in a fluidised-bed, Fuel 79 (2000) 873–883.
[13] M. Komatina, V. Manovic, D. Dakic, An experimental study of temperature of burning coal particle in fluidized bed, Energy and Fuels 20 (2006) 114–119.
[14] P.K. Agarwal, R.D. La Nauze, Transfer processes local to the coal particle: a review of drying, devolatilization and mass transfer in fluidized bed combustion, Chemical Engineering Research and Design 67 (1989) 457–480.
[15] J.F. Stubington, H. Guangwei, A.W. Scaroni, Devolatilization times of mm-size coal particles, Fuel 70 (1991) 1105–1108.
[16] S.N. Oka, Fluidized Bed Combustion, Marcel Dekker, New York, 2004.
[17] J.P.K. Peeler, H.J. Poynton, Devolatilization of large coal particles under fluidized bed conditions, Fuel 71 (1992) 425–430.
[18] S.S. Zabrodsky, Heat transfer between solid particles and a gas in a nonuniformly aggregated fluidized bed, International Journal of Heat and Mass Transfer 6 (1963) 23–31.
[19] J.F. Stubington, T.Y.S. Chui, S. Saisithidej, Experimental factors affecting coal devolatilization time in fluidized bed combustion, Fuel Science and Technology International 10 (1992) 397–419.
[20] J.F. Stubington, Sumaryono, Release of volatiles from large coal particles in a hot fluidized bed, Fuel 63 (1984) 1013–1019.
[21] J.Q. Zhang, H.A. Becker, R.K. Code, Devolatilization and combustion of large coal particles in a fluidized bed, Canadian Journal of Chemical Engineering 68 (1990) 1010–1017.
[22] J.F. Stubington, K.W.K. Ng, B. Moss, P.K. Peeler, Comparison of experimental methods for determining coal particle devolatilization times under fluidized bed combustor conditions, Fuel 76 (1997) 233–240.
[23] T.F. Salam, X.L. Shen, B.M. Gibbs, A technique for determining devolatilization rates of large coal particles in a fluidized bed combustor, Fuel 67 (1988) 414–419.
[24] D.B. Anthony, J.B. Howard, Coal devolatilization and hydrogasification, AIChE Journal 22 (1976) 625–656.
[25] A.S. Jamaluddin, J.S. Truelove, T.F. Wall, Devolatilization of bituminous coals at medium to high heating rates, Combustion and Flame 63 (1986) 329–337.
[26] J. Tomeczek, H. Palugniok, Specific heat capacity and enthalpy of coal pyrolysis at elevated temperatures, Fuel 75 (1996) 1089–1093.
[27] P. Arendt, K.-H. van Heek, Comparative investigations of coal pyrolysis under inert gas and H_2 at low and high heating rates and pressures up to 10 MPa, Fuel 60 (1981) 779–787.
[28] J.S. Chern, A.N. Hayhurst, Does a large coal particle in a hot fluidised bed lose its volatile content according to the shrinking core model? Combustion and Flame 139 (2004) 208–221.
[29] O. Levenspiel, Chemical Reaction Engineering, John Wiley, New York, 1999.
[30] R. Wong, E. Whittingham, A Comparison of combustion technologies for electricity generation, The Pembina Institute, Canada, 2006, p. 23.